

Nutrient limitation of phytoplankton growth in the central equatorial Pacific Ocean

Alyssa M. Biggs  
University of Washington  
School of Oceanography, Box 357940  
Seattle WA 98195  
ambiggs@uw.edu  
7 March 2024

## **Abstract**

Phytoplankton play a key role in removing carbon dioxide from Earth's atmosphere by ultimately exporting organic carbon to the deep ocean through the process known as the biological pump. Larger phytoplankton sink more rapidly than smaller, resulting in more carbon export as they are less likely to be fully remineralized. However, phytoplankton growth is highly dependent on the supply of key nutrients. In this study, I examined the effects of limiting nitrate, silicate, and iron on phytoplankton growth. To achieve this, I incubated samples from 4° S and 0° along the 167° W meridian for 96 hours in different nutrient treatments. I filtered subsamples of each incubation through a size-fractionated manifold every 24 hours and measured the chlorophyll  $\alpha$  concentrations in three different size fractions to determine growth rates. Growth rates were not statistically different between treatments across all size fractions at both 4° S and the equator, but growth rates did statistically differ between 4° S and the equator in most treatments. Nutrient analysis showed an N:P usage of  $15.0 \pm 0.93:1$  at 4° S and  $9.09 \pm 1.34:1$  at the equator, and an Si:P usage at 4° S of  $6.2 \pm 2.19:1$  over the control and nitrate-depleted treatments and  $1.74 \pm 0.10:1$  over the two silicate-depleted treatments; at the equator, these ratios were  $8.89 \pm 0.80:1$  over the control, nitrate-depleted, and iron-depleted treatments and  $3.81 \pm 0.78:1$  over the two silicate-depleted treatments. The results of this study suggest that controls on phytoplankton growth are more varied and complex than just nutrient availability, and more work is necessary to determine what actually limits growth in this area.

## **Plain Language Summary**

Phytoplankton are microscopic marine organisms that both supply oxygen to the atmosphere and remove carbon dioxide. They take up CO<sub>2</sub> to use in photosynthesis and incorporate the resulting

organic carbon into their biomass. When they die, they slowly sink into the deep ocean, and their organic carbon is eventually buried in sediment, effectively removing it from circulation. This process is known as the biological pump, and it is one of the critical atmospheric CO<sub>2</sub> removal mechanisms on Earth. Larger phytoplankton tend to sink more rapidly, meaning less of their biomass is consumed by other organisms during its descent. Understanding the limitations on phytoplankton growth is key to quantifying the biological pump and constraining one of the ways in which climate change will affect a future Earth. One of those limitations is the availability of key nutrients, specifically nitrate, silicate, and iron. This study aimed to determine which of these nutrients limits growth of phytoplankton communities from two different areas in the central equatorial Pacific Ocean. Samples of phytoplankton from 4° S and 0° along the 167° W meridian were grown for 96 hours in five different nutrient treatments. Subsamples were taken every 24 hours and chlorophyll *a* concentrations were measured to determine growth. No statistically significant difference was found in the growth rates between any treatments at both locations, and there were only a few differences between growth rates in the same treatment from different locations. Nutrient analysis showed that phytoplankton at 4° S used more NO<sub>3</sub> with respect to P compared to the equator, and samples from both locations used less silicate with respect to P in the silicate-depleted treatments. This suggests that it is not simply one nutrient that limits phytoplankton growth in these areas and that phytoplankton may be adapted to deal with low nutrient conditions.

## Introduction

Phytoplankton play a critical role in Earth's oceans, even beyond their function as the base of the marine food web. They produce around half of the world's oxygen and organic carbon by taking up inorganic carbon dioxide from the atmosphere to use in photosynthesis (Harris, 2012). The carbon that they fix is eventually exported to the deep ocean through excretion by their predators or by the sinking of dead phytoplankton. Once settled to the ocean floor, the carbon can be gradually sequestered in the sediment as it is buried by further sedimentation. It is this last function that is particularly crucial in this era of rapid climate change as entire industries seek ways to mitigate anthropogenic carbon emissions (National Academies of Sciences, Engineering, and Medicines, 2022).

Annually, the oceans remove up to 26% of CO<sub>2</sub> from the atmosphere (Friedlingstein et al., 2021). This inorganic carbon is taken up by phytoplankton and fixed into organic carbon, which eventually sinks into the deep ocean through the biological pump. The biological pump describes the set of biogeochemical processes by which inorganic carbon is transformed into organic carbon and cycled through the ocean to eventual sequestration (De La Rocha & Passow, 2014). One of the key components of the biological pump is the settling of biogenic particles, including dead phytoplankton. The velocity of these settling particles is described by Stoke's Law, equation (1),

$$W_s = (D^2 * (\rho_{\text{particle}} - \rho_{\text{water}}) * g) / 18\mu \quad (1)$$

where  $W_s$  is the settling velocity,  $D$  is the particle diameter,  $g$  is gravitational acceleration, and  $\mu$  is the viscosity of seawater, which varies with temperature but is equal to 0.00107 Pa\*s at 20°C. Thus, the diameter of a settling particle is key to how quickly it reaches the deep ocean, with larger particles settling more rapidly. Phytoplankton have a large size range, from picophytoplankton as small as 0.2  $\mu\text{m}$  to greater than 10  $\mu\text{m}$  (Sieburth et al., 1978). All sizes of phytoplankton contribute

significantly to the biological pump, but the larger the organism, the faster it will settle and the less likely it will be remineralized in its descent. Since most phytoplankton have a life span of just days, a high growth rate is essential to reaching these larger sizes.

One critical control on phytoplankton growth and cell size is nutrient concentration. In most of the ocean, the primary nutrient limiting growth is nitrate (Bristow et al., 2017). However, the equatorial Pacific is an area of high nitrate concentration but low chlorophyll concentrations (Edwards et al., 2004). Previous studies have suggested that the limiting nutrients in the eastern equatorial Pacific are iron and silicate rather than nitrate (Brzezinski et al., 2011). Phytoplankton require iron to synthesize chlorophyll and to produce a variety of enzymes, including nitrogenase for nitrogen fixation (Schoffman et al., 2016). Silicate is required to build cell walls (frustules), especially for larger phytoplankton like diatoms (Egge & Aksnes, 1992).

Though the equatorial Pacific is widely studied, most studies have been focused around 140°W and points further east. Data for the western and central equatorial Pacific is sparse. The Mercator-Pisces Biogeochemical Daily Forecast model, a biogeochemical model that projects biological productivity and daily dissolved nutrient concentrations at 1/4° resolution, shows that as of 7 Dec 2023, iron concentration maintains a consistent pattern from east to west, but silicate concentration is far lower in the central equatorial Pacific, especially at 5° S (Fig 1). Upwelling from the Equatorial Undercurrent supplies remineralized nutrients to the surface (Wyrki, 1981), but this current weakens during El Niño years and upwelling slows. The eastern equatorial Pacific likely receives both dissolved iron and dissolved silicate from riverine input, wind-blown dust, and sediment dissolution along continental margins (Horner et al., 2015; DeMaster, 1981), but the central equatorial Pacific is too far from major land areas to significantly benefit from these inputs. Iron remains consistent along the equator due to upwelling of deep-water iron from sources such as

hydrothermal vents (Horner et al., 2015). However, silicate is not as easily replenished, with upwelling accounting for less than 5% of the marine silicate supply (DeMaster, 1981).

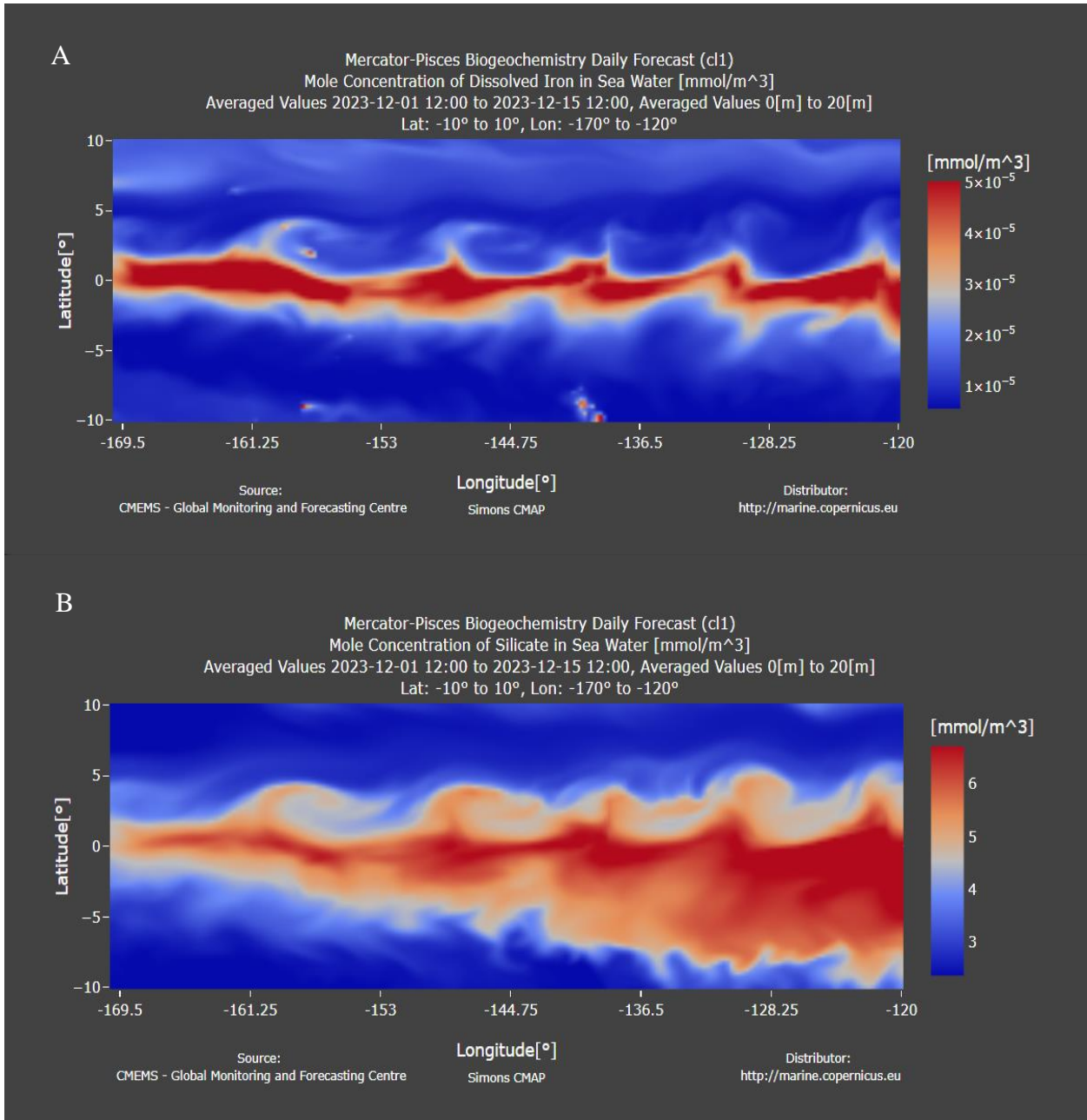


**Figure 1.** Heatmaps showing A) predicted dissolved iron in  $\text{mmol m}^{-3}$ ; and B) predicted silicate in  $\text{mmol m}^{-3}$  concentrations from  $170^\circ\text{W}$  to  $120^\circ\text{W}$  and  $10^\circ\text{S}$  to  $10^\circ\text{N}$ , averaged over the surface 20 m. Each map shows an average of two weeks of forecast, from 01 December 2023 to 15 December 2023. Visualization created with Simons CMAP using data from the Mercator-Pisces Biogeochemistry Daily Forecast.

Enrichment experiments have shown that with abundant iron, overall phytoplankton growth increases, but diatom cell division is limited by silicate availability. The co-addition of iron and silicate to an incubation resulted in an increase in cell density and cell division rates in diatoms larger than 20  $\mu\text{m}$  compared to both a control and an iron-only treatment (Marchetti et al., 2010). However, the growth of diatoms smaller than 20  $\mu\text{m}$  was optimized in an iron-only treatment compared to the iron and silicate treatment. This suggests that the growth of larger phytoplankton is co-limited by both iron and silicate, while smaller phytoplankton are more limited by iron only, as they can compensate for low silicate levels by producing thinner frustules (Brzezinski et al., 2011).

Picophytoplankton with diameters of less than 2.0  $\mu\text{m}$ , such as *Prochlorococcus* and *Synechococcus*, tend to dominate HNLC areas of the ocean. Larger diatoms have a higher metal requirement, especially in the equatorial Pacific (Twining & Baines, 2013), and they have less cell surface area compared to their volume to host the transporter proteins necessary for nutrient uptake. While the contribution of picophytoplankton to carbon export is not insignificant (Richardson & Jackson, 2007), it is the larger, rapidly-sinking diatoms which drive the biological pump, and it is nutrient availability that is a key driver of phytoplankton growth

This study examined the effects of limiting nitrate, iron, and silicate on chlorophyll  $\alpha$  growth in community samples from two different areas of the equatorial Pacific, one within the area of the Equatorial Undercurrent at  $0^\circ$  and one outside of it at  $4^\circ$  S. Based on the above-mentioned cell requirements and properties as well as the findings from Marchetti et al., I hypothesized that the growth of phytoplankton smaller than 10  $\mu\text{m}$  would be limited primarily by iron, while the growth of larger phytoplankton ( $>10$   $\mu\text{m}$ ) would be co-limited by both iron and silicate. I further hypothesized that the phytoplankton collected from  $0^\circ$  would have significantly more growth than the phytoplankton collected at  $4^\circ$  S, given the naturally higher nutrient concentrations at the equator.

## Methods

### *Community Sampling and Incubation*

All community sampling, incubations, and chlorophyll analysis was conducted aboard the *R/V Thomas G. Thompson* during cruise TN427 from 29 December 2023-10 January 2024. The first community sample was collected on 3 January 2024 at 4° S, 167° W (referred to as the 4° S sample), while the second community sample was collected on 4 January 2024 at 0°, 167° W (referred to as the 0° sample) (Fig 2). Both samples were obtained from 10 L Niskin bottles at a depth of 10 m and filtered through a 50 µm mesh to remove large particles and organisms. The water from the Niskin bottles was initially collected in dark bottles to prevent further photosynthesis, 12 bottles from the 4° S sample and 15 bottles from the 0° sample. A separate 1 L dark bottle was collected at each latitude to provide a t=0 measurement.

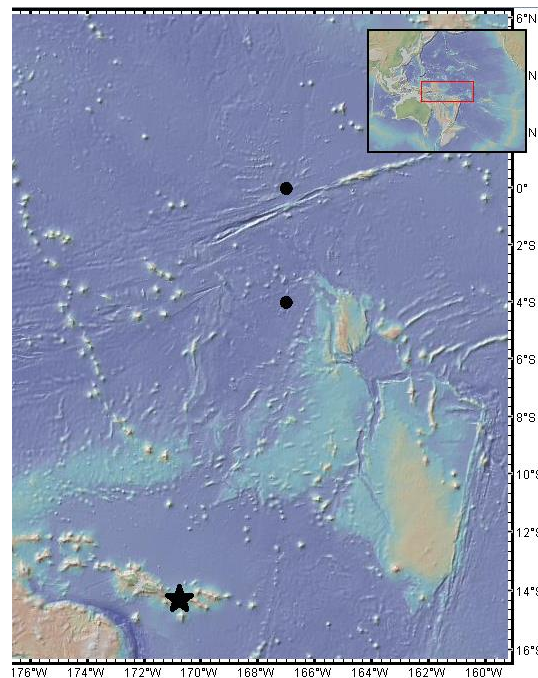


**Figure 2.** Map of sampling sites (black circles). The inset shows global position, and the black star indicates the port of Pago Pago, American Samoa.

Each sample except for the t=0 was transferred from the dark bottles to clear 1 L plastic bottles for incubation. Each incubation bottle was then spiked with nitrate, phosphate, iron, and/or silicate depending on the treatment (Table 1). One treatment was nutrient-replete as a control, while the other 4 treatments were nutrient-replete except for the intended limiting nutrient: one bottle that lacked silicate, one bottle that lacked iron, one bottle that lacked nitrate, and one bottle that lacked both iron and silicate. All treatments were prepared in triplicate; however, due to water volume limitations, a solely iron-deficient treatment was not prepared at 4° S. The treatment bottles were then placed in an on-deck incubator with screening to simulate the in-situ light level at 10 m. Temperature in the incubator was maintained by flowing seawater.

**Table 1.** Summary of incubation treatments and added nutrient concentrations

Sample location	Treatment	[NaNO <sub>3</sub> ] <sup>a</sup> (mmol/m <sup>3</sup> )	[NaH <sub>2</sub> PO <sub>4</sub> ·H <sub>2</sub> O] <sup>b</sup> (mmol/m <sup>3</sup> )	[Na <sub>2</sub> SiO <sub>3</sub> ·9H <sub>2</sub> O] <sup>c</sup> (mmol/m <sup>3</sup> )	[FeCl <sub>3</sub> ·6H <sub>2</sub> O] <sup>d</sup> (mmol/m <sup>3</sup> )
4° S	Control	1.09	0.5	3.28	5.7*10 <sup>-6</sup>
	Fe+Si+PO <sub>4</sub>	----	0.5	3.28	5.7*10 <sup>-6</sup>
	NO <sub>3</sub> +Fe+PO <sub>4</sub>	1.09	0.5	----	5.7*10 <sup>-6</sup>
	NO <sub>3</sub> +PO <sub>4</sub>	1.09	0.5	----	----
0°	Control	4.42	0.75	6.03	5.68*10 <sup>-5</sup>
	Fe+Si+PO <sub>4</sub>	----	0.75	6.03	5.68*10 <sup>-5</sup>
	NO <sub>3</sub> +Si+PO <sub>4</sub> <sup>e</sup>	4.42	0.75	6.03	----
	NO <sub>3</sub> +Fe+PO <sub>4</sub>	4.42	0.75	----	5.68*10 <sup>-5</sup>
	NO <sub>3</sub> +PO <sub>4</sub>	4.42	0.75	----	----

*Note.* A summary of the concentrations of added nutrient spikes for each 1L incubation treatment. All spike concentrations were based on in-situ seawater concentrations, obtained from the Mercator-PISCES Biogeochemical Daily Forecast using Simons CMAP. “----” indicates that this nutrient was not added to the bottle.

<sup>a</sup>5000 μM stock. <sup>b</sup>500 μM stock. <sup>c</sup>2000 μM stock. <sup>d</sup>500 nM stock. <sup>e</sup>Not performed at 4° S due to water volume limitations.

### *Chlorophyll Analysis*

Every 24 hours, each treatment bottle was briefly removed from the incubator and 250 mL of water was removed from the bottle as a subsample. Each subsample was filtered through a size-fractionated manifold using a vacuum pump. Three different Isopore polycarbonate filters were used in the manifold, with pore diameters of 10  $\mu\text{m}$ , 3  $\mu\text{m}$ , and 0.2  $\mu\text{m}$ . Combined with the initial mesh filtration during collection, this resulted in three size fractions—10-50  $\mu\text{m}$ , 3-10  $\mu\text{m}$ , and 0.2-3  $\mu\text{m}$ . Once filtration was complete, each filter was folded and inserted into a 15 mL centrifuge tube and topped with 10 mL of 90% acetone. The initial 24- and 48-hour samples from both 4° S and 0° were vortexed for 30 seconds. However, the vortex ceased functioning after this point, so all remaining samples were shaken vigorously by hand for 1 minute. The centrifuge tubes were then placed in a -20° C freezer for at least 24 hours (Mantoura & Llewellyn, 1983). This process of subsampling, filtration, extraction, and freezing was repeated every 24 hours for a total of 96 hours for all incubations. At the 96-hour mark, approximately 20 mL of water was removed from each bottle before filtration for nutrient measurement. Nutrient analysis was conducted on land at the University of Washington Marine Chemistry Lab using a Seal Analytical AA3 and following the protocols of the WOCE Hydrographic Program.

After at least 24 hours in the freezer, the centrifuge tubes with the acetone-extracted filters were removed from the freezer, shaken vigorously, and centrifuged at 3500 rpm for 10 minutes to pellet filter debris. The supernatant was transferred to a glass cuvette tube with a Pasteur pipet and fluorescence was measured using a Turner 7000 fluorometer ( $F_0$ ). A second measurement,  $F_a$ , was made after adding 3 drops of 10% HCl to convert all pigments into phaeopigments. These two measurements were then used to calculate chlorophyll  $\alpha$  concentrations using Equation (2):

$$\text{Chl } \alpha = K * (F_m / (F_m - 1)) * (F_0 - F_a) * (V_{\text{extracted}} / V_{\text{filtered}}) \quad (2)$$

where  $K$  and  $F_m$  are instrument-specific response factors and acidification coefficients (Lorenzen, 1966).

One-way analysis of variance (ANOVA) tests were performed to determine if there was any statistically significant difference in growth rates between the treatments and between the size fractions within the same treatment, and a student's t-test was used to compare treatments from the equator and 4° S.

## **Results**

### *Chlorophyll $\alpha$ Concentrations and Growth Rates*

Across all size fractions, chlorophyll  $\alpha$  increased over time following a slight initial decrease from  $t=0$  to  $t=24$  hrs (Fig 3 & 4). The measured change in chlorophyll was converted to a chlorophyll growth rate by plotting the natural log of the chlorophyll measurement over time, with the slope of the resulting line equaling the growth rate (Table 2).

**Table 2.** *Chlorophyll a* growth rates over 96 hours

Sample Location	Nutrients Added	Size Fraction ( $\mu\text{m}$ )	Chlorophyll $\alpha$ growth rate ( $\text{day}^{-1}$ )	R <sup>2</sup> Value	
4° S	Control (all nutrients)	10-50	$0.739 \pm 0.027$	$0.958 \pm 0.023$	
		3-10	$0.677 \pm 0.051$	$0.733 \pm 0.029$	
		0.2-3	$0.767 \pm 0.061$	$0.689 \pm 0.047$	
	Fe+Si+PO <sub>4</sub>	10-50	$0.686 \pm 0.241$	$0.963 \pm 0.023$	
		3-10	$0.588 \pm 0.186$	$0.736 \pm 0.204$	
		0.2-3	$0.619 \pm 0.249$	$0.717 \pm 0.300$	
	NO <sub>3</sub> +Fe+PO <sub>4</sub>	10-50	$0.674 \pm 0.082$	$0.908 \pm 0.068$	
		3-10	$0.723 \pm 0.016$	$0.753 \pm 0.020$	
		0.2-3	$0.745 \pm 0.028$	$0.748 \pm 0.018$	
	NO <sub>3</sub> +PO <sub>4</sub>	10-50	$0.783 \pm 0.165$	$0.817 \pm 0.264$	
		3-10	$0.776 \pm 0.117$	$0.742 \pm 0.048$	
		0.2-3	$0.794 \pm 0.080$	$0.776 \pm 0.054$	
	0°	Control (all nutrients)	10-50	$0.611 \pm 0.219$	$0.917 \pm 0.082$
			3-10	$0.247 \pm 0.177$	$0.403 \pm 0.329$
			0.2-3	$0.311 \pm 0.243$	$0.390 \pm 0.337$
Fe+Si+PO <sub>4</sub>		10-50	$0.688 \pm 0.133$	$0.895 \pm 0.041$	
		3-10	$0.469 \pm 0.068$	$0.663 \pm 0.013$	
		0.2-3	$0.470 \pm 0.016$	$0.632 \pm 0.042$	
NO <sub>3</sub> +Fe+PO <sub>4</sub>		10-50	$0.541 \pm 0.053$	$0.886 \pm 0.089$	
		3-10	$0.379 \pm 0.028$	$0.535 \pm 0.066$	
		0.2-3	$0.396 \pm 0.031$	$0.569 \pm 0.045$	
NO <sub>3</sub> +Si+PO <sub>4</sub>		10-50	$0.585 \pm 0.135$	$0.859 \pm 0.135$	
		3-10	$0.396 \pm 0.051$	$0.618 \pm 0.081$	
		0.2-3	$0.431 \pm 0.026$	$0.590 \pm 0.054$	
NO <sub>3</sub> +PO <sub>4</sub>		10-50	$0.333 \pm 0.068$	$0.724 \pm 0.049$	
		3-10	$0.321 \pm 0.018$	$0.486 \pm 0.021$	
		0.2-3	$0.315 \pm 0.117$	$0.442 \pm 0.166$	

*Note:* Indicated error is one standard deviation, n = 3 for each treatment.

In the 10-50  $\mu\text{m}$  size fraction at 4° S, the chl  $\alpha$  growth rate ranged from  $0.674 \pm 0.082 \text{ d}^{-1}$  in the silicate-depleted treatment to  $0.783 \pm 0.165 \text{ d}^{-1}$  in the joint iron- and silicate-depleted treatment. In the 3-10  $\mu\text{m}$  size fraction, the chl  $\alpha$  growth rate ranged from  $0.588 \pm 0.186 \text{ d}^{-1}$  in the nitrate-depleted treatment to  $0.776 \pm 0.117 \text{ d}^{-1}$  in the joint iron- and silicate-depleted treatment. In the 0.2-3

$\mu\text{m}$  size fraction, the growth rate ranged from  $0.619 \pm 0.249 \text{ d}^{-1}$  in the nitrate-depleted treatment to  $0.794 \pm 0.080 \text{ d}^{-1}$  in the joint iron- and silicate-depleted treatment (Fig 3). However, no statistically significant differences in growth rates were found between the treatments in any size fraction (one-way ANOVA test,  $p$ -values  $> 0.05$ ). Within the same treatment, no statistically significant difference was found between size fractions for any treatment (one-way ANOVA test,  $p$ -values  $> 0.05$ ).

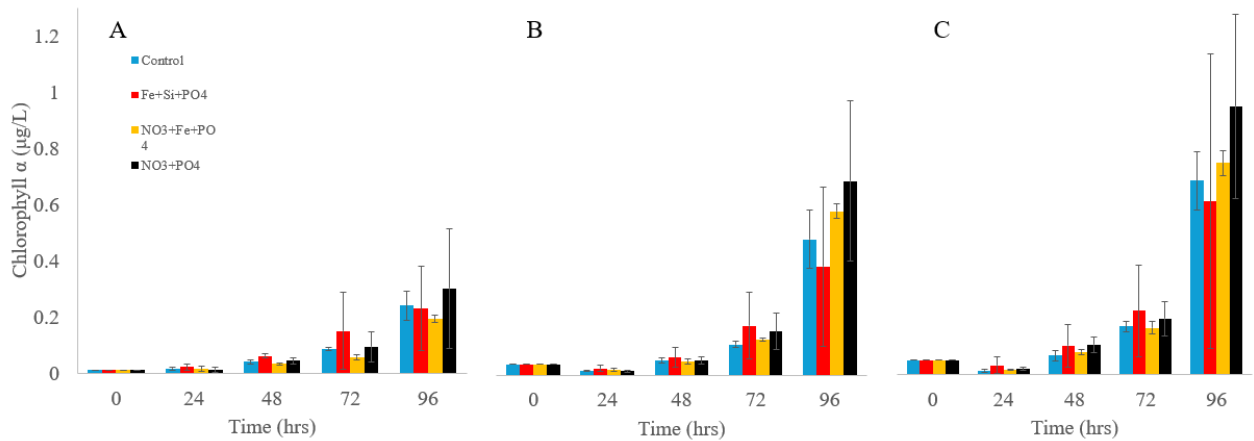


**Figure 3.** Chlorophyll  $\alpha$  concentrations over time from the  $4^\circ \text{ S}$  incubations. A) 10-50  $\mu\text{m}$ , B) 3-10  $\mu\text{m}$ , and C) 0.2-3  $\mu\text{m}$ . “Control” (blue bar) was amended with  $\text{NO}_3$ , Fe, Si, and  $\text{PO}_4$ ; “Fe+Si+ $\text{PO}_4$ ” (red bar) was amended with Fe, Si, and  $\text{PO}_4$ ; “ $\text{NO}_3$ +Fe+ $\text{PO}_4$ ” (gold bar) was amended with  $\text{NO}_3$ , Fe, and  $\text{PO}_4$ ; and “ $\text{NO}_3$ + $\text{PO}_4$ ” (black bar) was amended with  $\text{NO}_3$  and  $\text{PO}_4$ . All concentrations of added nutrients are provided in Table 1. All treatments were done in triplicate. Height of the bar is the average across all three replicates, error bars indicate one standard deviation.

In the 10-50  $\mu\text{m}$  size fraction at  $0^\circ$ , the chl  $\alpha$  growth rate ranged from  $0.333 \pm 0.068 \text{ d}^{-1}$  in the joint iron- and silicate-depleted treatment to  $0.688 \pm 0.133 \text{ d}^{-1}$  in the nitrate-depleted treatment. In the 3-10  $\mu\text{m}$  size fraction, the growth rate ranged from  $0.247 \pm 0.177 \text{ d}^{-1}$  in the control to  $0.469 \pm 0.068 \text{ d}^{-1}$  in the nitrate-depleted treatment. In the 0.2-3  $\mu\text{m}$  size fraction, the growth rate ranged from  $0.311 \pm 0.243 \text{ d}^{-1}$  in the control to  $0.470 \pm 0.016 \text{ d}^{-1}$  in the nitrate-depleted treatment (Fig 4). There was no statistically significant difference in growth rates between treatments in any size fraction

(one-way ANOVA test,  $p$ -values  $> 0.05$ ). Within the same treatment, only the nitrate-limited and silicate-limited treatments showed any statistically significant difference (one-way ANOVA test,  $p$ -values  $< 0.05$ ). In both cases, the 10-50  $\mu\text{m}$  size fraction had the highest growth rate when compared to the other two size fractions, despite having the overall lowest chlorophyll concentrations (Tukey post-hoc test,  $p$ -values  $< 0.05$ ). The 3-10  $\mu\text{m}$  and 0.2-3  $\mu\text{m}$  size fractions were statistically equivalent when compared to one another (Tukey post hoc test,  $p$ -values  $> 0.05$ ).

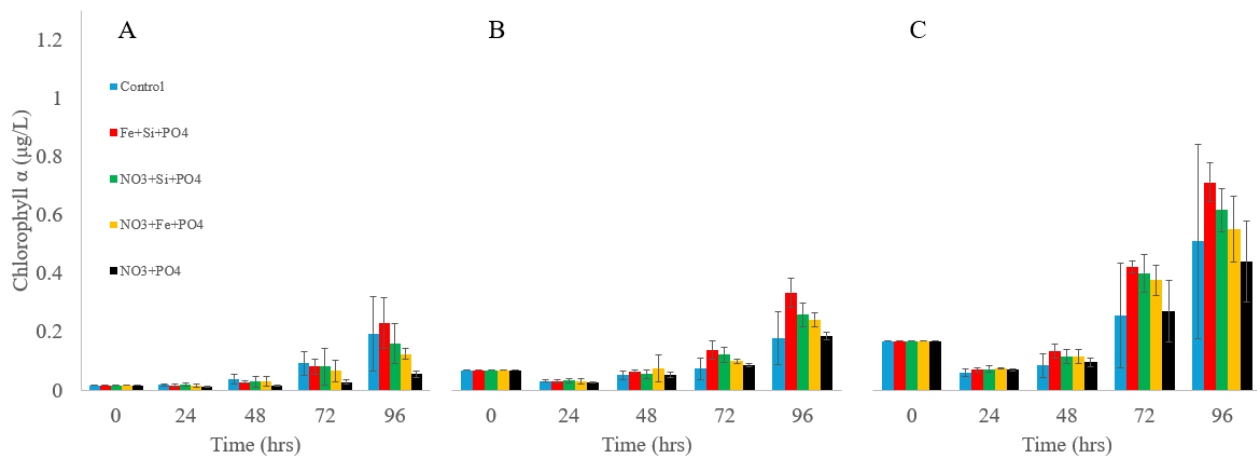


**Figure 4.** Chlorophyll  $\alpha$  concentrations over time from the  $0^\circ$  incubations. A) 10-50  $\mu\text{m}$ , B) 3-10  $\mu\text{m}$ , and C) 0.2-3  $\mu\text{m}$ . “Control” (blue bar) was amended with  $\text{NO}_3$ , Fe, and Si; “Fe+Si+ $\text{PO}_4$ ” (red bar) was amended with Fe, Si, and  $\text{PO}_4$ ; “ $\text{NO}_3$ +Si+ $\text{PO}_4$ ” (green bar) was amended with  $\text{NO}_3$ , Si, and  $\text{PO}_4$ ; “ $\text{NO}_3$ +Fe+ $\text{PO}_4$ ” (gold bar) was amended with  $\text{NO}_3$ , Fe, and  $\text{PO}_4$ ; and “ $\text{NO}_3$ + $\text{PO}_4$ ” (black bar) was amended with  $\text{NO}_3$  and  $\text{PO}_4$ . All concentrations of added nutrients are provided in Table 1. All treatments were done in triplicate. Height of the bar is the average across all three replicates, error bars indicate one standard deviation.

Between the  $4^\circ$  S and the equator, only the joint iron- and silicate-depleted treatment had significantly different growth rates in the 10-50  $\mu\text{m}$  size fraction (t-test,  $p$ -value  $< 0.05$ ). In the 3-10  $\mu\text{m}$  size fraction, the control, silicate-depleted, and joint iron- and silicate-depleted treatments all statistically differed between  $4^\circ$  S and the equator, with the equator treatments experiencing less average growth (t-test,  $p$ -value  $< 0.05$  for the differing treatments). In the 0.2-3  $\mu\text{m}$  size fraction, the control, silicate-depleted, and the joint iron- and silicate-depleted treatment statistically differed

between the two locations, again with the equator treatment experiencing less growth (t-test, p-value < 0.05 for the differing treatments).

### *Nutrient Depletion*

In all treatments, nutrients decreased from t=0 to t=96 hrs (Table 3). The ratios of N:P usage at 4° S averaged  $15.0 \pm 0.93:1$  over all treatments and averaged  $9.09 \pm 1.34:1$  over all treatments at the equator. The ratio of Si:P usage at 4° S averaged  $6.2 \pm 2.19:1$  over the control and nitrate-depleted treatments and averaged  $1.74 \pm 0.10:1$  over the two silicate-depleted treatments. At the equator, the ratio of Si:P usage averaged  $8.89 \pm 0.80:1$  over the control, nitrate-depleted, and iron-depleted treatments and averaged  $3.81 \pm 0.78:1$  over the two silicate-depleted treatments.

**Table 3.** *Nutrient concentrations over time*<sup>a</sup>

Sample Location	Treatment	[PO <sub>4</sub> ], initial <sup>b</sup> (mmol/m <sup>3</sup> )	[PO <sub>4</sub> ], final (mmol/m <sup>3</sup> )	[Si(OH) <sub>4</sub> ], initial (mmol/m <sup>3</sup> )	[Si(OH) <sub>4</sub> ], final (mmol/m <sup>3</sup> )	[NO <sub>3</sub> ], initial (mmol/m <sup>3</sup> )	[NO <sub>3</sub> ], final (mmol/m <sup>3</sup> )
4° S	Control	0.87 ± 0.04	0.67 ± 0.02	4.43 ± 0.17	3.50 ± 0.05	3.14 ± 0.49	0.39 ± 0.17
	Fe+Si+PO <sub>4</sub>	0.87 ± 0.04	0.75 ± 0.53	4.43 ± 0.17	3.50 ± 0.23	2.05 ± 0.49	0.19 ± 0.09
	NO <sub>3</sub> +Fe+PO <sub>4</sub>	0.87 ± 0.04	0.71 ± 0.06	1.15 ± 0.17	0.86 ± 0.03	3.14 ± 0.49	0.60 ± 0.43
	NO <sub>3</sub> +PO <sub>4</sub>	0.87 ± 0.04	0.69 ± 0.04	1.15 ± 0.17	1.45 ± 1.04	3.14 ± 0.49	0.47 ± 0.35
0°	Control	1.24 ± 0.04	1.00 ± 0.08	8.48 ± 0.77	6.23 ± 0.25	6.96 ± 0.38	5.05 ± 1.06
	Fe+Si+PO <sub>4</sub>	1.24 ± 0.04	0.96 ± 0.02	8.48 ± 0.77	5.87 ± 0.14	2.54 ± 0.38	0.18 ± 0.09
	NO <sub>3</sub> +Fe+PO <sub>4</sub>	1.24 ± 0.04	1.00 ± 0.04	2.45 ± 0.77	1.67 ± 0.71	6.96 ± 0.38	4.28 ± 1.03
	NO <sub>3</sub> +Si+PO <sub>4</sub>	1.24 ± 0.04	0.95 ± 0.07	8.48 ± 0.77	6.17 ± 0.07	6.96 ± 0.38	4.15 ± 0.77
	NO <sub>3</sub> +PO <sub>4</sub>	1.24 ± 0.04	0.99 ± 0.06	2.45 ± 0.77	1.36 ± 0.04	6.96 ± 0.38	4.91 ± 0.30

*Note:* Nutrient concentrations as measured at t=0 and t=96 hrs, averaged across the three replicants for each treatment. Errors are one standard deviation.

<sup>a</sup>Fe concentrations were not measured. <sup>b</sup>Initial concentrations determined by adding concentration of nutrients in unamended seawater averaged through the mixed layer (data collected by AJ Carothers) and nutrient spikes from Table 1.

## **Discussion**

Based on the statistical tests performed, there is no significant difference in growth rates between any of the treatments from 4° S or the equator. Within the same treatment, only the nitrate-limited and silicate-limited treatments from the equator had significant differences, with the 10-50 µm size fraction experiencing the highest growth rate. These results are inconclusive with respect to this study's original hypothesis, which was that the growth of phytoplankton larger than 10 µm would be co-limited by iron and silicate, and the growth of phytoplankton smaller than 10 µm would be limited by iron. The growth rates of all treatments were equivalent across all treatments in all size fractions, so I am not able to say with certainty which nutrients actually limit growth in phytoplankton of any size in this region. The results also refute the second part of the hypothesis, which was that treatments from the equator would grow more rapidly than treatments from 4° S. In all cases where growth was significantly different between the two locations, the incubations from the equator experienced less average growth than those from 4° S.

Nutrient analysis suggests that phytoplankton can adapt to low-nutrient conditions by changing the amount of nutrients they require, if those are the general conditions they live in. At both 4° S and the equator, the ratio of Si:P usage was much lower in all size fractions of the silicate-depleted treatments compared to the silicate-replete treatments. However, growth was consistent and statistically equivalent across all treatments. This suggests that phytoplankton of all sizes in both areas may be adapted to deal with low-silicate conditions by utilizing less silicate overall, confirming previous findings (Brzezinski et al., 2011). However, the N:P usage ratios differed widely between the equator and 4° S, with a lower ratio at the equator. The Pacific is currently experiencing an El Niño cycle, which slows the Equatorial Undercurrent and decreases nutrient upwelling. Given that El Niño is a recurring cycle, phytoplankton from this region might have adaptations to deal with widely varying nutrient supply, including slowing their growth and using

less nitrate. At the equator, the nitrate-depleted treatments had the greatest chlorophyll concentrations across all size fractions, with relatively small standard deviations. Conversely, the nitrate-depleted treatments at 4° S had the lowest chlorophyll concentrations with a wide standard deviation. This suggests that phytoplankton from the equator may be more able to deal with low nitrate concentrations.

The results of this study suggest that controls on phytoplankton growth in all size categories are more complex and varied than a single or even two nutrients. One of the most significant indicators of this finding is the growth of the control treatments. If nutrient supply was the sole or even primary control on phytoplankton growth, one would expect that a fully nutrient-replete treatment would experience the most growth regardless of size or origin. However, that was not the case in this study. There was no statistically significant difference between the control treatment and any of the other treatments at either location. In absolute numbers, the control treatments had lower growth rates than most of the other treatments across all size fractions and origins. This likely indicates additional unaccounted-for factors controlling growth.

## **Conclusions**

Overall, the results of this study were inconclusive regarding which nutrients limit phytoplankton growth across various size categories in the equatorial Pacific. Though some differences existed between communities from within the Equatorial Undercurrent and outside of it, growth rates were statistically equivalent both between different treatments in the same size fraction, and different size fractions within the same treatment, with very few exceptions. This suggests that phytoplankton from these areas have adaptations that allow them to continue to grow

despite low nutrient conditions. Future studies could investigate other potential growth limiters such as grazing and viruses, or use additional mesh filtration to isolate one or more specific size fractions and more accurately target limiting nutrients for different-sized phytoplankton. Ultimately, more work is necessary to constrain the controls on the biological pump in this area, which will improve our understanding of this important part of our planet's climate system in a time of rapid change.

### **Acknowledgements**

I would like to thank the captain and crew of the *R/V Thomas G. Thompson* during cruise TN427 for their invaluable assistance, support, and hard work. I would also like to thank the instructors of the OCEAN 443/444/445 classes at the University of Washington, especially Dr. Ginger Armbrust, for their mentorship and guidance through this entire study, as well as my fellow classmates for their moral support, cheerleading, and making sure I took breaks. Finally, I would like to thank the University of Washington School of Oceanography for funding this research.

## References

- Bristow, L. A., Mohr, W., Ahmerkamp, S., & Kuypers, M. M. M. (2017). Nutrients that limit growth in the ocean. *Current Biology*, 27(11), R474–R478.  
<https://doi.org/10.1016/j.cub.2017.03.030>
- Brzezinski, M. A., Baines, S. B., Balch, W. M., Beucher, C. P., Chai, F., Dugdale, R. C., et al. (2011). Co-limitation of diatoms by iron and silicic acid in the equatorial Pacific. *Deep Sea Research Part II: Topical Studies in Oceanography*, 58(3–4), 493–511.  
<https://doi.org/10.1016/j.dsr2.2010.08.005>
- De La Rocha, C. L., & Passow, U. (2007). Factors influencing the sinking of POC and the efficiency of the biological carbon pump. *Deep Sea Research Part II: Topical Studies in Oceanography*, 54(5–7), 639–658. <https://doi.org/10.1016/j.dsr2.2007.01.004>
- DeMaster, D. J. (1981). The supply and accumulation of silica in the marine environment. *Geochimica et Cosmochimica Acta*, 45(10), 1715–1732. [https://doi.org/10.1016/0016-7037\(81\)90006-5](https://doi.org/10.1016/0016-7037(81)90006-5)
- Edwards, A. M., Platt, T., & Sathyendranath, S. (2004). The high-nutrient, low-chlorophyll regime of the ocean: Limits on biomass and nitrate before and after iron enrichment. *Ecological Modelling*, 171(1–2), 103–125. <https://doi.org/10.1016/j.ecolmodel.2003.06.001>
- Egge, J., & Aksnes, D. (1992). Silicate as regulating nutrient in phytoplankton competition. *Marine Ecology Progress Series*, 83, 281–289. <https://doi.org/10.3354/meps083281>
- Friedlingstein, P., Jones, M. W., O’Sullivan, M., Andrew, R. M., Bakker, D. C. E., Hauck, J., et al. (2022). Global Carbon Budget 2021. *Earth System Science Data*, 14(4), 1917–2005.  
<https://doi.org/10.5194/essd-14-1917-2022>

- Harris, G. (1986). *Phytoplankton ecology: structure, function, and fluctuation*. Berlin: Springer.
- Horner, T. J., Williams, H. M., Hein, J. R., Saito, M. A., Burton, K. W., Halliday, A. N., & Nielsen, S. G. (2015). Persistence of deeply sourced iron in the Pacific Ocean. *Proceedings of the National Academy of Sciences*, *112*(5), 1292–1297. <https://doi.org/10.1073/pnas.1420188112>
- Lorenzen, C. J. (1966). A method for the continuous measurement of in vivo chlorophyll concentration. *Deep-Sea Research*, *13*, 223–227. [https://doi.org/10.1016/0011-7471\(66\)91102-8](https://doi.org/10.1016/0011-7471(66)91102-8)
- Mantoura, R. F. C., & Llewellyn, C. A. (1983). The rapid determination of algal chlorophyll and carotenoid pigments and their breakdown products in natural waters by reverse-phase high-performance liquid chromatography. *Analytica Chimica Acta*, *151*, 297–314. [https://doi.org/10.1016/S0003-2670\(00\)80092-6](https://doi.org/10.1016/S0003-2670(00)80092-6)
- Marchetti, A., Varela, D. E., Lance, V. P., Johnson, Z., Palmucci, M., Giordano, M., & Armbrust, E. V. (2010). Iron and Silicic Acid Effects on Phytoplankton Productivity, Diversity, and Chemical Composition in the Central Equatorial Pacific Ocean. *Limnology and Oceanography*, *55*(1), 11–29. <http://www.jstor.org/stable/20622858>
- National Academies of Sciences, Engineering, and Medicine. 2022. A Research Strategy for Ocean-based Carbon Dioxide Removal and Sequestration. Washington, DC: The National Academies Press. <https://doi.org/10.17226/26278>
- Richardson, T. L., & Jackson, G. A. (2007). Small Phytoplankton and Carbon Export from the Surface Ocean. *Science*, *315*(5813), 838–840. <https://doi.org/10.1126/science.1133471>
- Schoffman, H., Lis, H., Shaked, Y., & Keren, N. (2016). Iron–Nutrient Interactions within Phytoplankton. *Frontiers in Plant Science*, *7*, 1223. <https://doi.org/10.3389/fpls.2016.01223>

- Sieburth, J. McN., Smetacek, V., & Lenz, J. (1978). Pelagic ecosystem structure: Heterotrophic compartments of the plankton and their relationship to plankton size fractions 1. *Limnology and Oceanography*, 23(6), 1256–1263. <https://doi.org/10.4319/lo.1978.23.6.1256>
- Twining, B. S., & Baines, S. B. (2013). The Trace Metal Composition of Marine Phytoplankton. *Annual Review of Marine Science*, 5(1), 191-215. <https://doi.org/10.1146/annurev-marine-121211-172322>
- Wyrski, K. (1981). An Estimate of Equatorial Upwelling in the Pacific. *Journal of Physical Oceanography*, 11(9), 1205–1214. [https://doi.org/10.1175/1520-0485\(1981\)011<1205:AEOEUI>2.0.CO;2](https://doi.org/10.1175/1520-0485(1981)011<1205:AEOEUI>2.0.CO;2)